

# Four-Electron Reduction of Diazo Compounds at a Single Tungsten Metal Center: A Theoretical Study of the Mechanism

Feliu Maseras,<sup>†,§</sup> Mark A. Lockwood,<sup>‡</sup> Odile Eisenstein,<sup>\*,†</sup> and Ian P. Rothwell<sup>\*,‡</sup>

Contribution from the Laboratoire de Structure et Dynamique des Systèmes Moléculaires et Solides, UMR 5636, Case Courrier 14, Université de Montpellier II, 34095 Montpellier cedex 5, France, and Department of Chemistry, 1393 Brown Building, Purdue University, West Lafayette, Indiana 47907-1393

Received November 20, 1997. Revised Manuscript Received April 27, 1998

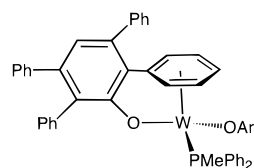
**Abstract:** A possible mechanism for the unprecedented one-metal reduction of diazobenzene by the  $[W(OC_6HPh_3-\eta^6-C_6H_5)(OAr)(PMe_2Ph)]$  ( $OAr = 2,3,5,6$ -tetraphenyl-oxide) complex was characterized by hybrid Becke3LYP DFT calculations on the model system  $[W(OH)_2(C_6H_6)(Ph_3)] + N_2H_2$ . The model reaction is shown to be strongly exothermic, and takes place via a multistep process with moderate activation energy barriers. We discuss how this specific set of ancillary ligands permits the reaction to occur on a one-metal system in place of the more usual two-metal systems.

## Introduction

The four-electron reductive cleavage of dioxygen and iso-electronic diazo double bonds by transition metal species is an important process which is usually carried out by species containing two metal centers.<sup>1–3</sup> Processes taking place at a single metal center are rare.<sup>4</sup> We recently provided evidence of such activity in the case of the  $[W(OC_6HPh_3-\eta^6-C_6H_5)(OAr)(PMe_2Ph)]$  ( $OAr = 2,3,5,6$ -tetraphenyl-oxide) complex.<sup>5</sup> The formally  $d^4$  W(II) metal center is stabilized by an  $\eta^6$  interaction with the *o*-phenyl ring of one of the aryloxy ligands (Chart 1). The complex reacts with  $O_2$  and a variety of  $RN=NR$  molecules to produce the corresponding bis(oxo) and bis(imido) derivatives. Reactions with asymmetric diazo substrates  $RN=NR'$  show conclusively that the reaction is intramolecular and that the four-electron oxidation or reduction is achieved on a single metal center.

The factors which make this reaction possible on a single metal center are still unclear since other systems react in a different manner.<sup>6</sup> A qualitative molecular orbital analysis suggested that the cleavage of the diazo compound by the  $d^4$   $[W(OAr)_2]$  fragment would be allowed by symmetry.<sup>5</sup> However, there is no obvious explanation as to how this presumably

## Chart 1



high-energy transition metal unsaturated fragment could be formed in the reactive media. Other aspects of the reaction such as the initial coordination of diazobenzene to the metal or the role of the phosphine and benzene ligands which are lost during the reaction are also not well understood.

In this paper, we present an analysis with the density functional theory (DFT) Becke3LYP method<sup>7</sup> on the model system  $[W(OH)_2(C_6H_6)(OAr)(Ph_3)]$  (**1**) +  $HN=NH$ , with the  $\eta^6$  coordinating benzene of one of the alkoxy groups represented as an independent ligand. A number of stationary points, intermediates, and transition states have been located on the potential hypersurface, resulting in a detailed mechanistic proposal that explains why this system is an efficient four-electron reducing agent.

## Computational Details

Ab initio calculations were carried out on the model system  $[W(OH)_2(C_6H_6)(Ph_3)] + HN=NH$  using the hybrid Becke3LYP density functional<sup>7</sup> as implemented in Gaussian 94.<sup>8</sup> The basis set was of valence double- $\zeta$  quality for all atoms. For tungsten<sup>9</sup> and phosphorus<sup>10</sup> we used the LANL2DZ effective core potential; for all other atoms we used the standard 6-31G basis.<sup>11</sup>

(7) (a) Becke, A. D. *J. Chem. Phys.* **1993**, *98*, 5648. (b) Lee, C.; Yang, W.; Parr, R. G. *Phys. Rev. B* **1988**, *37*, 785. (c) Stephens, P. J.; Devlin, F. J.; Chabalowski, C. F.; Frisch, M. J. *J. Phys. Chem.* **1994**, *98*, 11623.

(8) Frisch, M. J.; Trucks, G. W.; Schlegel, H. B.; Gill, P. M. W.; Johnson, B. G.; Robb, M. A.; Cheeseman, J. R.; Keith, T.; Petersson, G. A.; Montgomery, J. A.; Raghavachari, K.; Al-Laham, M. A.; Zakrzewski, V. G.; Ortiz, J. V.; Foresman, J. B.; Peng, C. Y.; Ayala, P. Y.; Chen, W.; Wong, M. W.; Andres, J. L.; Replogle, E. S.; Gomperts, R.; Martin, R. L.; Fox, D. J.; Binkley, J. S.; Defrees, D. J.; Baker, J.; Stewart, J. P.; Head-Gordon, M.; Gonzalez, C.; Pople, J. A. *Gaussian 94*; Gaussian, Inc.: Pittsburgh, PA, 1995.

(9) Hay, P. J.; Wadt, W. R. *J. Chem. Phys.* **1985**, *82*, 299.

(10) Wadt, W. R.; Hay, P. J. *J. Chem. Phys.* **1985**, *82*, 284.

\* E-mail: eisenst@lsd.univ-montp2.fr, rothwell@chem.purdue.edu.

<sup>†</sup> Université de Montpellier II.

<sup>‡</sup> Purdue University.

<sup>§</sup> Present address: Unitat de química Física, Edifici C.n; Universitat Autònoma de Barcelona, 08193 Bellaterra, Catalonia, Spain.

(1) (a) Cotton, F. A.; Duraj, S. A.; Roth, W. J. *J. Am. Chem. Soc.* **1984**, *106*, 4749. (b) Hill, J. E.; Profflet, R. D.; Fanwick, P. E.; Rothwell, I. P. *Angew. Chem., Int. Ed. Engl.* **1990**, *29*, 664. (c) Hill, J. E.; Fanwick, P. E.; Rothwell, I. P. *Inorg. Chem.* **1991**, *30*, 1143.

(2) (a) Bryan, J. C.; Mayer, J. M. *J. Am. Chem. Soc.* **1990**, *112*, 2298. (b) Laplaza, C. E.; Cummins, C. C. *Science* **1995**, *268*, 861. (c) Laplaza, C. E.; Odom, A. L.; Davis, W. M.; Cummins, C. C.; Protasiewicz, J. D. *J. Am. Chem. Soc.* **1995**, *117*, 4999. (d) Legzdins, P.; Young, M. A.; Batchelor, R. J.; Einstein, F. W. B. *J. Am. Chem. Soc.* **1995**, *117*, 8798. (e) Lee, S. Y.; Bergman, R. G. *J. Am. Chem. Soc.* **1995**, *117*, 5877. (f) Laplaza, C. E.; Johnson, M. J. A.; Peters, J. C.; Odom, A. L.; Kim, E.; Cummins, C. C.; George, G. N.; Pickering, I. J. *J. Am. Chem. Soc.* **1996**, *118*, 8623.

(3) Cui, Q.; Musaev, D. G.; Svensson, M.; Sieber, S.; Morokuma, K. *J. Am. Chem. Soc.* **1995**, *117*, 12366.

(4) (a) Arney, D. S. J.; Burns, C. J. *J. Am. Chem. Soc.* **1995**, *117*, 9448.

(5) Lockwood, M. A.; Fanwick, P. E.; Eisenstein, O.; Rothwell, I. P. *J. Am. Chem. Soc.* **1996**, *118*, 2762.

(6) Brown, S. N.; Mayer, J. M. *J. Am. Chem. Soc.* **1993**, *31*, 4091.

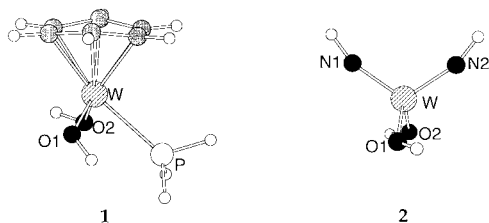


**Figure 1.** Optimized Becke3LYP geometries of the reactant  $[\text{W}(\text{OH})_2(\text{C}_6\text{H}_6)(\text{PH}_3)]$  (**1**) and of the product  $[\text{W}(\text{OH})_2(\text{NH})_2]$  (**2**).

**Table 1.** Selected Geometrical Parameters (Å and deg) from the Becke3LYP Geometry Optimization of the Model System,  $[\text{W}(\text{OH})_2(\text{C}_6\text{H}_6)(\text{PH}_3)]$  (**1**), Compared with X-ray Data for  $[\text{W}(\text{OC}_6\text{HPh}_3-\eta^6-\text{C}_6\text{H}_5)(\text{OAr})(\text{PMe}_2\text{Ph})]^a$

	calcd	exptl		calcd	exptl
W–P	2.556	2.479	X–W–P	131.5	130.1
W–O	1.977	1.994	X–W–O	119.8	118.3
W–C	2.327	2.244	W–O–H(C) <sup>b</sup>	120.3	125.3
W–X1	1.834	1.746	O–W–X1–P	105.0	106.8
O–W–O	114.0	115.2	O–W–X1–O	150.0	146.4

<sup>a</sup> Average values are presented for parameters involving the oxygen atoms of the alkoxy ligands, and for the carbon atoms of the benzene ligand. X1 stands for a dummy atom in the center of the benzene ring. <sup>b</sup> H in the computed model system, C in the experimental system.

All stationary points were optimized with analytical first derivatives using the standard default convergence criteria in Gaussian 94. Transition states were located using approximate Hessians and synchronous transit-guided quasi-Newton methods.<sup>12</sup> In doubtful cases, the nature of the local minima connected through a certain transition state was checked by reoptimizing from slightly distorted transition state geometries. Most of the intermediates were located in this way.

## Reactant and Product

Comparison of the optimized geometries of our models for reactant and product with available X-ray structures provides a test of the validity of the computational method. The optimized geometry of  $[\text{W}(\text{OH})_2(\text{C}_6\text{H}_6)(\text{PH}_3)]$  (**1**) is shown in Figure 1, and selected geometrical parameters are given and compared with the X-ray structure<sup>13</sup> of  $[\text{W}(\text{OC}_6\text{HPh}_3-\eta^6-\text{C}_6\text{H}_5)(\text{OAr})(\text{PMe}_2\text{Ph})]$  in Table 1. The overall agreement between computed and experimental geometries is good. The largest discrepancy (0.083 Å) is found for the W–C(benzene) distance which could be related to the intrinsic difficulty in estimating metal–arene bond distances as well as to some oversimplification in our calculated model. In particular the lack of an intramolecular bridge between one of the alkoxides and the benzene ring removes a geometrical constraint which could enforce the close proximity between the ring and the metal in the experimental system. The complex has a three-legged piano-stool geometry, but these legs are coordinated in a highly asymmetrical manner. If X1 is the center of the benzene ring, the dihedral angles O–W–X1–O (experimental, 146.4°; computed, 150.0°) and O–W–X1–P (experimental, 106.8°; computed, 105.0°) are very different. The geometry of the complex is far from the symmetric arrangement of a “regular” three-legged piano stool (dihedral angles of 120.0°), and closer to that of a regular four-legged piano stool (dihedral angles of 90.0, 180.0°) with one missing ligand. The empty site which is trans to the phosphine ligand will serve to accept the incoming diazo group. The distorted piano-stool

(11) Hehre, W. J.; Ditchfield, R.; Pople, J. A. *J. Chem. Phys.* **1972**, *56*, 2257.

(12) Peng, C.; Ayala, P. Y.; Schlegel, H. B.; Frisch, M. J. *J. Comput. Chem.* **1996**, *17*, 49.

(13) Lockwood, M. A.; Fanwick, P. E.; Rothwell, I. P. *Polyhedron* **1995**, *14*, 3363.

**Table 2.** Selected Geometrical Parameters (Å and deg) from the Becke3LYP Geometry Optimization of the Model System,  $[\text{W}(\text{OH})_2(\text{NH})_2]$  (**2**), Compared with X-ray Data for  $[\text{W}(\text{OAr})_2(\text{NPh})_2]^a$

	calcd	exptl		calcd	exptl
W–O	1.905	1.917	O–W–N	108.6	107.0
W–N	1.762	1.739	W–O–H(C) <sup>a</sup>	134.4	134.2
O–W–O	111.3	119.8	W–N–H(C) <sup>a</sup>	160.9	165.3
N–W–N	111.4	108.4			

<sup>a</sup> Average values are presented for parameters involving oxygen and nitrogen atoms. Experimental values presented are averaged between the nonequivalent molecules present in the unit cell. <sup>b</sup> H in the computed model system, C in the experimental system.

geometry is associated with the unsaturated nature of the complex. Keeping in mind that the benzene takes three coordination sites, a regular piano-stool complex must be pseudooctahedral. When the number of electrons at the metal is less than six, geometrical distortion away from an octahedral environment is expected and thus away from a regular piano-stool geometry. In the present case, the unsaturation in complex **1** is made possible by the two strongly  $\pi$ -donating alkoxide ligands.<sup>14</sup>

The optimized geometry of  $[\text{W}(\text{OH})_2(\text{NH})_2]$  (**2**) (Figure 1, Table 2) is very close to the crystal structure<sup>5</sup> of  $[\text{W}(\text{OAr})_2(\text{NPh})_2]$ . The discrepancy between experimental and calculated bond distances is less than 0.03 Å, and the overall tetrahedral geometry is properly reproduced. The deviation of the O–W–O angle (experimental, 119.8°) away from the exact tetrahedral coordination is probably associated with the steric bulk of the alkoxide groups. This distortion is not present in the model structure. The computed geometry has  $C_2$  symmetry, with the symmetry axis bisecting the O–C–O angle. This symmetry is broken by the bulkier substituents in the experimental system. The angles at N and O are well reproduced with a clearly bent alkoxide ligand (W–O–H angle of 134.4°), and a much more linear imido ligand (W–N–H angle of 160.9°). This follows chemical expectations that an imido ligand is a more potent  $\pi$  donor than an alkoxide group in this W(VI) complex. The higher oxidation state of the metal in **2** compared to **1** results in W–O bonds which are shorter than those in the reactants by 0.072 Å, and in a W–O–H angle which is larger by 14°.

The reaction is highly exothermic. The energy of **1** plus a free model diazo compound diazene<sup>15</sup>  $\text{HN}=\text{NH}$  is 130.2 kcal/mol above that of **2** +  $\text{C}_6\text{H}_6$  +  $\text{PH}_3$ . The large exothermicity is, however, not unprecedented for this type of reaction. Brown and Mayer<sup>6</sup> estimated an exothermicity of more than 70 kcal/mol in the four-electron oxidation from the peroxo compound  $(\text{HBpz}_3)\text{ReO}(\text{O}_2)$  to the trioxo compound  $(\text{HBpz}_3)\text{ReO}_3$ . However, they found that, despite the large exothermicity, the reaction did not proceed through a one-metal mechanism in their system. It is therefore of interest to understand what makes a one-metal reaction possible in the present system. This will be done in the following by a discussion of the reaction path.

## General Energy Profile

Figure 2 presents the computed energy profile for the multistep reaction going from **1** +  $\text{HN}=\text{NH}$  to **2** +  $\text{C}_6\text{H}_6$  +  $\text{PH}_3$ . Species **3**, **5**, **7**, **9**, and **11** are local minima in the potential hypersurface, corresponding to intermediates on the reaction path. Species **4**, **6**, **8**, **10**, and **12** are transition states.

(14) Caulton, K. G. *New J. Chem.* **1994**, *18*, 25.

(15) The reactant diazene  $\text{HN}=\text{NH}$  is assumed to be in the cis form because this is best suited for the reaction, even if the trans isomer is more stable by 7.0 kcal/mol at this computational level.

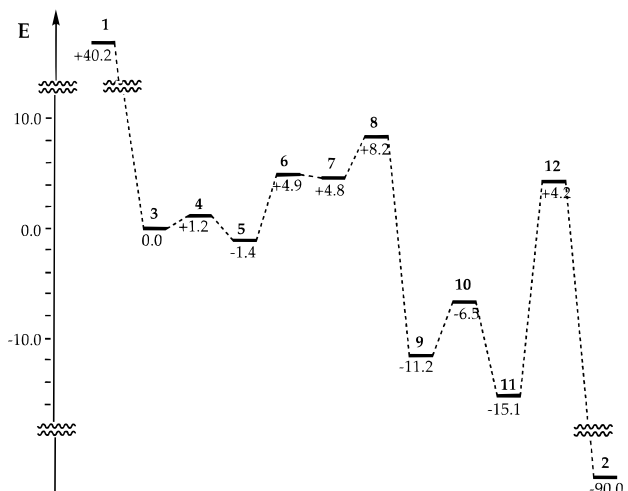


**Figure 2.** Potential energy profile (kcal/mol) from the reactants  $[[\text{W}(\text{OH})_2(\text{C}_6\text{H}_6)(\text{PH}_3)]]$  (**1**) +  $\text{HN}=\text{NH}$  to the products  $[[\text{W}(\text{OH})_2(\text{NH})_2]$  (**2**) +  $\text{C}_6\text{H}_6$  +  $\text{PH}_3$ ].

One of the most remarkable features is how far apart in energy the reactants (**1** +  $\text{HN}=\text{NH}$ ) and products (**2** + benzene +  $\text{PH}_3$ ) are from the other species. While complexes **3–12** span a range of 23.3 kcal/mol, **1** remains 32.0 kcal/mol above the highest energy structure of the **3–12** group, and **2** lies 74.9 kcal/mol below the lowest of them. Most of this complicated reaction mechanism consists therefore in an essentially isoenergetic process necessary to go from intermediates **3–11**, with only this last intermediate able to give the much more stable product **2**. A number of gradual changes take place during the reaction: the oxidation state of W goes from II to IV and then to VI; the benzene ligand goes from being bound in an  $\eta^6$  mode to the metal, to an  $\eta^2$  coordination, before being released; the diazo species is initially coordinated in a monohapto way ( $\eta^1$ ), before going dihapto ( $\eta^2$ ), and finally cleaving to give rise to two  $\text{W}=\text{N}$  bonds; the phosphine ligand is lost at an early stage of the reaction.

The overall reaction can be viewed, and will be analyzed as a gradual change in the formal oxidation state of the metal, coupled with that of the entering diazo group. Of course, this is just an arbitrary way to label the steps of the reaction, since our assignment of oxidation states relies on the assumption that the metal–ligand interaction is purely of a donor–acceptor type. An alternative view, considering the fact that the  $\text{W}=\text{N}$  bonds of the product are more covalent than the  $\text{W}-\text{P}$  bond of the reactant, might be more realistic, but would be less intuitive.

Despite the large number of intermediates, none of them have been seen in the experimental study. This may be due to the relatively low activation energies during the reaction and the very strong thermodynamic drive to products. We now proceed to discuss the consecutive steps (i) initial  $\eta^1$  coordination of  $\text{HN}=\text{NH}$ , (ii) change from  $\eta^1$   $\text{HN}=\text{NH}$  to  $\eta^2$   $\text{HN}=\text{NH}^{2-}$ , and (iii) change from  $\eta^2$   $\text{HN}=\text{NH}^{2-}$  to  $\text{HN}=\text{W}=\text{NH}$ .

### Initial $\eta^1$ Coordination of $\text{HN}=\text{NH}$

In the first step of the reaction, the diazene molecule  $\text{HN}=\text{NH}$  binds to the 16-electron reactant **1** to give the 18-electron species **3**  $[[\text{W}(\text{OH})_2(\text{C}_6\text{H}_6)(\eta^1\text{-HN}=\text{NH})(\text{PH}_3)]]$ , a species that loses the phosphine ligand to produce the 16-electron species **5**  $[[\text{W}(\text{OH})_2(\text{C}_6\text{H}_6)(\eta^1\text{-HN}=\text{NH})]$ . Species **4** is the transition state between **3** and **5**. The oxidation state of the metal remains unchanged as  $\text{W}(\text{II})$ ,  $d^4$ , throughout this section of the reaction path. The geometries of these three species are shown in Figure 3, with selected geometrical parameters collected in Table 3.

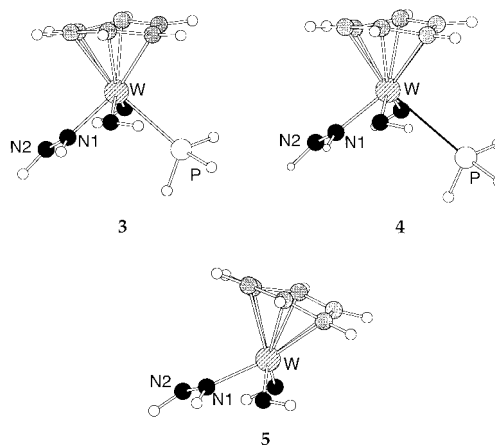


**Figure 3.** Optimized Becke3LYP geometries for species **3**, **4**, and **5** concerning the initial  $\eta^1$  coordination of  $\text{HN}=\text{NH}$ .

**Table 3.** Selected Geometrical Parameters (Å and deg) from the Becke3LYP Geometry Optimization of Species Related to the Initial Coordination of the Diazeno Molecule to the Reactant Species **1**

	<b>1</b>	<b>3</b>	<b>4</b>	<b>5</b>
W–N1		2.006	1.993	1.986
W–N2		2.998	2.969	2.941
N1–N2	1.256	1.306	1.312	1.313
W–N1–N2		128.4	126.7	124.9
W–P	2.556	2.631	3.045	
W–C(shortest)	2.270	2.247	2.200	2.218
W–C(longest)	2.422	2.476	2.495	2.525

Complex **3** has a regular four-legged piano-stool structure, with the four basal ligands occupying essentially equivalent sites. The diazene and phosphine ligands are in transoid positions as expected from the geometry of **1**. Species **5** is a three-legged piano stool with three asymmetrically positioned legs as in **1**. In fact, **5** results from the replacement in **1** of  $\text{PH}_3$  by  $\text{HN}=\text{NH}$ . The reaction has gone through an associative mechanism, where  $\text{PH}_3$  and  $\text{HN}=\text{NH}$  bind simultaneously to the metal (**3**). A dissociative mechanism would involve a 14-electron intermediate which, although reported in some specific cases,<sup>16</sup> should not be thought of as the more likely route.

Replacement of  $\text{PH}_3$  by  $\text{HN}=\text{NH}$  (comparing **1** +  $\text{HN}=\text{NH}$  to **5** +  $\text{PH}_3$ ) is exothermic by 41.6 kcal/mol. The high  $\sigma$ -donor capability and the presence of a donating  $\pi$ -donor orbital in  $\text{HN}=\text{NH}$  makes it a much better candidate than  $\text{PH}_3$  to stabilize a 16-electron species. The exothermicity is also apparent in the geometrical parameters of **3**. The  $\text{W}-\text{P}$  distance of 2.631 Å is far from the equilibrium distance of 2.556 Å found in **1**, while  $\text{W}-\text{N1}$ , 2.006 Å, is much closer to its equilibrium value of 1.986 Å in **5**. In other words,  $\text{PH}_3$  is a better departing group than  $\text{HN}=\text{NH}$  from **3**. Another side effect of the large exothermicity is the lack of a transition state between **1** and **3**. According to our calculations, the addition of  $\text{HN}=\text{NH}$  to **1** should proceed without activation energy. The slightly greater stability (1.2 kcal/mol) of the 16-electron species **5** with respect to the 18-electron species **3** is probably associated with the presence of three strong  $\pi$ -donors, which destabilize a saturated complex through 4-electron repulsion between the lone pairs of the ligands and the occupied nonbonding d orbitals on the metal but are beneficial to an unsaturated species.<sup>14</sup>

The early departure of the phosphine ligand can explain the influence of added phosphine to the reactive media. It has been shown<sup>5</sup> that an excess of phosphine inhibits the reaction, but

(16) Cooper, A.C.; Streib, W.E.; Eisenstein, O. Caulton, K. G. *J. Am. Chem. Soc.* **1997**, *119*, 9069.

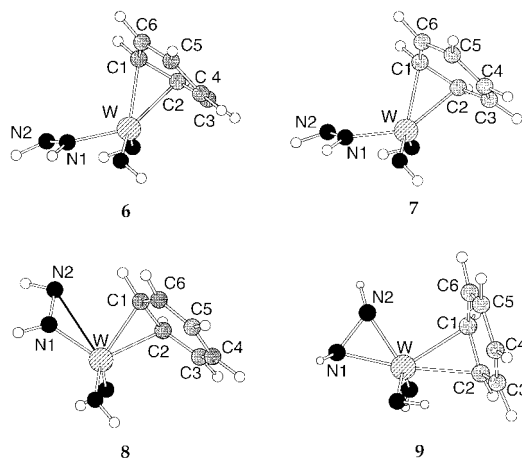


**Figure 4.** Optimized Becke3LYP geometries for species **6**, **7**, **8**, and **9** concerning the transit from  $\eta^1$  to  $\eta^2$  coordination of  $\text{HN}=\text{NH}$ .

**Table 4.** Selected Geometrical Parameters (Å and deg) from the Becke3LYP Geometry Optimization of Species Related to the Transformation from  $\eta^1$  to  $\eta^2$  Coordination of  $\text{HN}=\text{NH}^a$

	<b>5</b>	<b>6</b>	<b>7</b>	<b>8</b>	<b>9</b>
W–N1	1.986	1.952	1.942	1.919	2.000
W–N2	2.941	2.945	2.939	2.760	1.966
N1–N2	1.313	1.330	1.337	1.355	1.478
W–C1,C2 <sup>a</sup>	2.312	2.200	2.180	2.169	2.274
W–C3,C6 <sup>a</sup>	2.439	2.786	2.925	3.047	3.188
W–C4,C5 <sup>a</sup>	2.407	3.088	3.409	3.628	3.805
N2–N1–W–X2	94.3	94.5	96.9	130.0	172.3

<sup>a</sup> X2 corresponds to a dummy atom on the bisector of the O–W–O angle. <sup>b</sup> Average of two values.

does not revert it. The impossibility of reversing the reaction is obvious from the energy profile of Figure 2, since the reverse reaction would have to overcome a barrier of more than 90.0 kcal/mol. The inhibition mechanism by added phosphine can be explained simply by its effect on the position of the equilibrium between **3** and **5**.

The  $\eta^1$  coordination of the diazo ligand throughout this part of the reaction is apparent, with a short W–N1 distance around 2.0 Å and a long W–N2 distance around 3.0 Å. The N1–N2 distance in species **3**, **4**, and **5** is about 1.31 Å, longer than that in free  $\text{HN}=\text{NH}$  (1.256 Å), but still well within the range expected for an N=N double bond. The benzene remains in an  $\eta^6$  coordination, with W–C bond distances in the range 2.200–2.525 Å.

#### From $\eta^1 \text{HN}=\text{NH}$ to $\eta^2 \text{HN}=\text{NH}^{2-}$

The next phase of the redox process is the  $\eta^2$  coordination of the diazo ligand. To make this possible, the benzene ligand has to partially decoordinate to liberate additional coordination sites. The  $\eta^1\text{-HN}=\text{NH}/\eta^6\text{-C}_6\text{H}_6$  complex **5** discussed in the previous section evolves therefore to the  $\eta^1\text{-HN}=\text{NH}/\eta^2\text{-C}_6\text{H}_6$  intermediate **7**. From **7**, the second nitrogen of diazene approaches the metal, resulting in the  $\eta^2\text{-HN}=\text{NH}/\eta^2\text{-C}_6\text{H}_6$  complex **9**. Structures **6** and **8** are transition states connecting **5** to **7**, and **7** to **9**, respectively. All these species are presented in Figure 4.

The reaction path can be followed through the geometrical parameters collected in Table 4. In going from **5** to **7** the three pairs of W–C distances (W–C1,C2; W–C3,C6; W–C4,C5) change from being quite similar in the  $\eta^6\text{-C}_6\text{H}_6$  complex **5**, with a difference of only 0.127 Å between them, to being clearly different in the  $\eta^2\text{-C}_6\text{H}_6$  complex **7**, with a difference of 1.224 Å between them. The situation in transition state **6** is intermediate, with a difference of 0.888 Å. The coordination

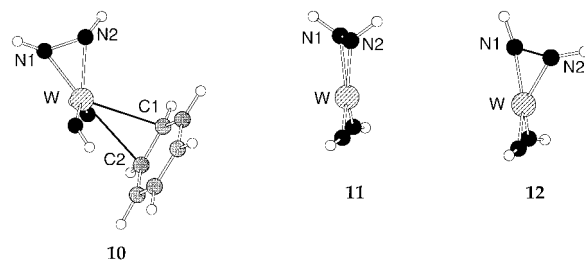


**Figure 5.** Optimized Becke3LYP geometries for species **10**, **11**, and **12** concerning the transit from  $\eta^2$  coordination of  $\text{HN}=\text{NH}$  to the formation of product **2**.

of  $\text{HN}=\text{NH}$  remains essentially unchanged until species **7**, with a difference of *ca.* 1.0 Å between W–N1 and W–N2. Drastic changes in the coordination mode of  $\text{HN}=\text{NH}$  occurs during the transformation of **7** to **9**. In this latter complex, the W–N1 and W–N2 distances differ by only 0.034 Å and  $\text{HN}=\text{NH}$  is clearly bonded in a dihapto manner. The transition state **8** shows an intermediate situation (2.760 *vs* 1.919 Å). In this step, the reaction coordinate seems to involve mostly the N2–N1–W–X2 dihedral angle, with a more gradual change in going from **7** (96.9°) to **8** (130.0°) to **9** (172.3°). This dihedral angle accounts for the fact that the O–O and N1–N2 vectors, essentially parallel until **7**, become almost perpendicular in **9**. In contrast the elongation of the N–N bond occurs after the transition state as shown in Table 4.

From the point of view of the formal metal coordination, **5** is a 16-electron W(II) complex, **7** is a 12-electron W(II) species, and **9** is a 12-electron W(IV) complex. In this step, there is consequently a formal transfer of two electrons from the metal to the diazene. For this formal count, we assume that the  $\eta^2$ -coordinated diazene is in a four-electron donor  $\text{HN}=\text{NH}^{2-}$  form. This seems to be in good agreement with the N1–N2 distance in **9** (1.478 Å), corresponding to a single N–N bond which has increased by 0.17 Å from that in **7**. It also accounts nicely for the energy profile presented in Figure 2. There is an energy loss of 6.2 kcal/mol in going from **5** to **7**, due to the loss of hapticity of benzene. This loss is largely compensated in **9**. Thus, **9**, despite being formally a 12-electron complex, is sufficiently stabilized by four  $\pi$ -donor ligands (the two oxygens and the two nitrogens).

#### From $\eta^2 \text{HN}=\text{NH}^{2-}$ to $\text{HN}=\text{W}=\text{NH}$

The last part of the reaction consists in the second two-electron transfer from W to the diazo group, resulting in the full oxidative cleavage of the N–N bond. This process is also preceded by the loss of the last weakly bound ligand from the coordination sphere. The benzene ligand leaves the  $\eta^2\text{-HN}=\text{NH}/\eta^2\text{-C}_6\text{H}_6$  complex **9** discussed above to produce the  $[\text{W}(\text{OH})_2(\eta^2\text{-HN}=\text{NH})]$  species **11**. Species **10** is the transition state between **9** and **11** (Figure 5). Finally, **11** evolves through transition **12** to the final diimido product  $[\text{W}(\text{OH})_2(\text{NH})_2(\text{NH})_2]$  (**2**).

There are more geometrical changes associated with the transformation from **9** to **11** than the mere departure of benzene. The N,N couple goes to a trans position with respect to the O,O couple (X2–W–X3 changing from 131.2° to 180.0° (Table 5), where X2 and X3 are the midpoints of the O–O and N–N vectors, respectively), and the N1–N2 bond rotates almost 90° with respect to the W–X3 axis. Interestingly, this latter change takes place mostly after the transition state **10**. Intermediate **11** can be seen as a heavily distorted square planar complex because of the presence of a bond between the two nitrogen atoms resulting in a small N1–W–N2 angle of 46.3°. Similarly to the product **2**, **11** has  $C_2$  symmetry. However, the transfor-

**Table 5.** Selected Geometrical Parameters (Å and deg) from the Becke3LYP Geometry Optimization of Species Related to the Transformation from  $\eta^2$  HN=NH<sup>2-</sup> to HN=W=NH<sup>a</sup>

	<b>9</b>	<b>10</b>	<b>11</b>	<b>12</b>	<b>2</b>
W–N1	2.006	1.944	1.951	1.841	1.762
W–N1–H	117.2	135.1	132.7	144.8	160.5
W–N2	1.969	2.017	1.951	1.958	1.762
W–N2–H	130.9	121.6	132.7	125.8	160.5
N1–N2	1.489	1.477	1.532	2.019	2.911
N1–W–N2	44.0	43.7	46.3	64.1	111.4
W–C1,C2 <sup>b</sup>	2.215	2.754			
X2–W–X3	131.2	161.5	180.0	170.5	180.0

<sup>a</sup> X2 and X3 correspond to dummy atoms on the bisectors of the O–W–O and N–W–N angles, respectively. <sup>b</sup> Average of two values.

mation from the square planar complex **11** to the tetrahedral complex **2** does not go via a symmetrical path. Transition state **12** is clearly asymmetric; the W–N1 double bond (W–N1, 1.841 Å; W–N1–H, 144.8°) is much more formed than the W–N2 double bond (W–N2, 1.958 Å; W–N2–H, 125.8°).

In this last phase of the reaction, the 12-electron W(IV) complex **9** is converted to the 10-electron W(IV) complex **11**, and then finally transformed into the 12-electron W(VI) product **2**. The 10-electron species is stabilized by the strong  $\pi$  donation from the alkoxide and diazo ligands. The second and last transfer of two electrons from the metal to the diazo group is completed in the last step, with the necessary preamble of the formation of **11**. In this last stage, the oxidation reaction is preceded by the loss of a ligand (departure of the dihapto-coordinated benzene). The energy profile (Figure 2) for this last phase of the reaction is quite interesting. The transformation from **9** to **11** is almost isoenergetic (–3.9 kcal/mol), with a low barrier (4.7 kcal/mol), while the step from **11** to **2** is amazingly exothermic (–74.9 kcal/mol), with a respectable activation barrier (19.3 kcal/mol). The whole multistep process, with the initial departure of the phosphine and the gradual departure of the  $\eta^6$  benzene ligand results in the formation without high energy cost of complex **11**. This complex with no other ligands has to go through the highest single-step barrier of the whole reaction path to reach the much more stable product. It is therefore quite clear that this reaction would not take place in systems with less labile ancillary ligands. The alkoxide ligands also play a crucial role of electron reservoirs able to adapt to the metal electronic environment. This behavior is certainly at the heart of many transformations in the presence of transition metal systems, and could be responsible for the rich alkoxide/aryloxide chemistry of metals in high oxidation states.

### Mathematical Characterization of the Stationary Points

In view of the complexity of the potential energy surface, the use of approximate Hessians in our calculations may raise some questions as to the reliability of our characterization of the various stationary points. Because of the presence of pseudopotentials, calculations of the full Hessian matrix must be done numerically (which is somewhat time consuming), as methods for its analytical computation<sup>17</sup> are not yet implemented in commercial programs. A full characterization of the stationary points would yield two main results: the number of negative eigenvalues and zero-point energy corrections. The latter could modify the energy profile by at most 5.0 kcal/mol, which although it might eliminate some of the intermediates, is clearly insufficient to modify the global picture.

The number of negative Hessian eigenvalues determines the nature of the stationary points as local minima, transition states,

or higher order stationary points. We are confident of the assignments we have made because (i) no symmetry constraints were imposed during the geometry optimizations, (ii) the quality of the approximate Hessians was improved via numerical calculation of important selected Hessian elements, and (iii) our assignments are logical and give a fully consistent reaction scheme.

As an additional check, we did compute the full Hessian for transition state **8**, which is the highest point in the potential energy surface. Diagonalization gave a single negative eigenvalue, with an imaginary frequency of 129.7 i cm<sup>-1</sup>. The associated transition vector corresponds to the expected motion of the noncoordinated N2 center and its associated H atom toward the metal. The nature of this point as a transition state and the nature of the process taking place are thus fully confirmed.

A second point of concern in our proposed reaction scheme is the precise connectivity between transition states and local minima. As previously mentioned, we have checked our reaction profile by reoptimizing starting from slightly distorted transition state geometries. Full confirmation of the connectivity by carefully following the intrinsic reaction coordinate (IRC)<sup>18</sup> downhill to reactants and products, respectively, is beyond our current computational resources.

As a final comment, it should be mentioned that a more important approximation lies in the nature of the model chosen for the calculations. The replacement of several substituents by hydrogen atoms and the absence of an intramolecular bridge between oxygen and benzene constitutes a source of inaccuracy probably more serious than any discussed above, its importance being currently impossible to estimate. The confidence we have in our results comes from the fact that each step is chemically significant.

### Conclusions

Calculations on the model system [W(OH)<sub>2</sub>(C<sub>6</sub>H<sub>6</sub>)(PH<sub>3</sub>)] + HN=NH with the Becke3LYP method yield a detailed mechanistic picture of the experimental reaction between [W(OC<sub>6</sub>-HPh<sub>3</sub>- $\eta^6$ -C<sub>6</sub>H<sub>5</sub>)(OAr)(PMe<sub>2</sub>Ph)] and PhN=NPh that satisfactorily explains the experimental observations. The reaction takes place through a multistep process, with no less than five consecutive transition states having been located. The progressive strengthening of the interaction of the RN=NR group with W is shown to be directly associated with the gradual loss of other ligands. The initial  $\eta^1$  coordination of RN=NR implies the loss of the phosphine, the subsequent step to  $\eta^2$  coordination involves the evolution from  $\eta^6$ -C<sub>6</sub>R<sub>6</sub> to  $\eta^2$ -C<sub>6</sub>R<sub>6</sub>, and the final oxidation of the N–N bond requires the full departure of benzene. Each loss of a ligand is compensated by the formation of a multiple bond between the metal and the potent electron donor alkoxide ligands. The unusual ability of the [W(OC<sub>6</sub>-HPh<sub>3</sub>- $\eta^6$ -C<sub>6</sub>H<sub>5</sub>)(OAr)(PMe<sub>2</sub>Ph)] complex to lose gradually, and at a relatively low energy cost, several ligands because of the compensating influence of the remaining ligands, which are potent electron donors, is at the heart of this reaction. Because of this combination of factors, the metal can donate up to four electrons and thus cleave N=N in diazo compounds or the O–O bond in dioxygen. This is the key to the original reactivity of complex **1** with dioxygen and isoelectronic diazo compounds.

**Acknowledgment.** The authors thank the Université de Montpellier 2, the CNRS (OE), and the NSF (IAP) for financial support. F.M. thanks the CNRS for the position of Associate Researcher.

JA973977L

(17) Cui, Q.; Musaev, D. G.; Svensson, M.; Morokuma, K. *J. Phys. Chem.* **1996**, *100*, 10936.

(18) Fukui, K. *Acc. Chem. Res.* **1981**, *14*, 363.